

Low-energy K -shell Compton scattering

E. G. Drukarev,¹ A. I. Mikhailov,² and I. A. Mikhailov^{2,3}

¹Max-Planck Institute für Physik Komplexer Systeme, D-01187 Dresden, Germany

²Petersburg Nuclear Physics Institute Gatchina, St. Petersburg, 188300 Russia

³University of Central Florida 4000 Central Florida Boulevard, Orlando, Florida 32816, USA

(Received 20 April 2010; published 4 August 2010)

We calculate the photon energy distribution and the total cross section for the Compton scattering on the K electrons for the case when the photon wave length is much smaller than the size of the K shell. We show that at the energies of the order of the binding energy I of the K electron most part of the spectrum is governed by the low-energy behavior. The total cross section has a local maximum at the energies $(1.5-2)I$, reaching the values of the order 1 barn. At higher photon energies the spectrum curves have two maxima, corresponding to low-energy ejected photons or electrons. The cross sections in the whole region are calculated. The actual calculations are carried out employing the nonrelativistic Coulomb functions, thus being valid for the single-electron atoms. However, the main features of the analysis are expected to be true for many-electron ions and neutral atoms. The results of the present analysis may be useful in calculations of the laser-induced and laser-assisted processes.

DOI: 10.1103/PhysRevA.82.023404

PACS number(s): 32.80.Aa, 32.80.Fb

I. INTRODUCTION

Theoretical investigations of the Compton scattering on bound electrons started many decades ago [1] and are going on until now [2]. The latest developments are reviewed in [3]. The earlier calculations focused on the case, when the outgoing electron obtained the nonrelativistic energies [4]. Later much attention was devoted to the Compton scattering of hard photons, causing the ejection of relativistic electrons [5]. These calculations were reviewed in [6]. Most of the experiments on the photon scattering have been focused on the case of the hard photon scattering on the targets with large nuclear charge Z [7]. Recent development of the methods for measuring the Compton scattering on bound electrons [8] is expected to provide new data. Construction of new powerful lasers stimulated studies of ionization processes. Experiments with the photons carrying the energies up to several keV are going on or are planned [9]. This motivates a more detailed analysis of interaction of the photons with the internal atomic shells [10,11]. On the other hand, the theory of nonrelativistic Compton scattering from the bound electrons is not complete yet.

The nonrelativistic Hamiltonian of interaction between the photons and electrons is

$$H = -e \frac{\mathbf{A} \cdot \mathbf{p}}{mc} + e^2 \frac{\mathbf{A}^2}{2mc^2}. \quad (1)$$

To obtain the amplitude of the Compton scattering one should include the first term of the Hamiltonian in the second-order perturbation theory. This provides the pole terms. The second term should be included in the first order, providing the “seagull” terms, known also as the A^2 terms. The early calculations were restricted to the seagull term, which is the only one that contributes in the nonrelativistic approximation in the case of free electrons [4,12,13]. It was noted, however [14], that the seagull terms are quenched when the wave length of the photon becomes much larger than the size of the bound state, and thus the pole terms should be included at lower photon energies.

Calculations of the pole terms are much more complicated, since they involve the propagator of the atomic electrons. These calculations were focused on the case of the hydrogenlike atoms. The general expressions for the amplitude of the Compton scattering from the K -shell electrons of a hydrogenlike atom were obtained in [14–18]. These authors use different representations of the nonrelativistic Coulomb Green functions. In these papers, the amplitude was presented in terms of special functions or their integral representations. Although paper [19] contained some numerical data on the amplitudes and triple differential cross sections, consistent computations of the energy distributions and cross sections have not been carried out yet.

In the present paper, we calculate the energy distributions and total cross sections of the nonrelativistic Compton scattering from the K electrons of the hydrogenlike atoms with the charge of the nucleus Z . We use the system of units with $\hbar = c = 1$. In these units the binding energy of the K electron is $I = \eta^2/2m$, with m denoting the electron mass, $\eta = m\alpha Z$ has the meaning of averaged momentum of the K electron, and $\alpha = 1/137$ is the fine structure constant. The incoming photon is characterized by the energy ω_1 and momentum \mathbf{k}_1 , $k_1 = \omega_1$. In a similar way for the ejected photon, $k_2 = \omega_2$. We consider the nonrelativistic case $\omega_1 \ll m$ and $(\alpha Z)^2 \ll 1$.

We employ the approach, developed in [17], where the explicit expression for the nonrelativistic Coulomb propagator in momentum space [20] has been used. Equations of [17] need additional evaluation before they can be used for the computations. This was done in [21], where they were used for calculation of the two-photon ionization of an atom. The amplitude of the Compton scattering can be obtained from that of the latter process by changing the sign of the linear momentum of the ejected photon \mathbf{k}_2 and of the energy ω_2 .

Until the ratio ω_1/I is of the order of unity, the amplitude is dominated by the pole terms. For all Z the amplitudes and the differential cross sections are expressed in terms of variables $x_{1(2)} = \omega_{1(2)}/I$ and are presented by universal functions of these parameters, thus the corresponding amplitudes $F_p(\omega_i, Z)$

are indeed the functions of the ratios $x_{1(2)} = \omega_{1(2)}/I$ [14]. The same refers to the cross section $\sigma(\omega_1, Z) = \sigma(x_1)$. We calculate these “universal” (scaled) functions for the energy distributions of the ejected photons and for the cross sections. For these energies the seagull term is quenched by a small factor of the order $\omega_1^2/\eta^2 \sim (\alpha Z)^2$ [14] being thus of the order of relativistic corrections to the pole terms.

The situation changes if we go to larger values of $\omega_1 \gg I$. The role of the seagull contributions increases. The seagull terms provide the main contribution to the energy distribution of the ejected photons $d\sigma/d\omega_2$ in the region $\omega_1 - \omega_2 \sim I$, corresponding to the low energy of ejected electrons $\varepsilon \sim I$, while the rest of the spectrum is dominated by the pole terms. Note that the seagull terms depend on the scaled variables $x_{1(2)}$ and on the nuclear charge Z separately.

We shall restrict ourselves to the case,

$$\omega_1 \ll \eta, \quad (2)$$

in other words, the wavelength of the incoming photon is much larger than the size of the bound state. The case of larger photon energies is well studied—see [3] and references therein. Under condition (2) the seagull and pole terms do not interfere. Thus, the energy distribution can be written as

$$\frac{d\sigma(\omega_1, \omega_2)}{d\omega_2} = \frac{d\sigma_P(\omega_1, \omega_2)}{d\omega_2} + \frac{d\sigma_{SG}(\omega_1, \omega_2)}{d\omega_2}, \quad (3)$$

with the lower indices P and SG denoting the contributions of the pole and seagull terms correspondingly. Since the first term on the right-hand side of Eq. (3) depends on the ratios $x_i = \omega_i/I$, while the second one depends also on Z , the total distribution (3) does not scale and depends on both x_i and Z . We shall see that in the energy region (1) the distribution $\frac{1}{Z^2} \frac{d\sigma_{SG}(\omega_1, \omega_2)}{d\omega_2}$ depends only on x_1 and x_2 .

At certain value of $x_1 = \tilde{x}_1$, estimated as $\tilde{x}_1 \sim 1/(\alpha Z)^{2/5}$, $\omega_1 \sim \eta(\alpha Z)^{3/5}$, the contribution of the seagull terms to the total cross section becomes equal to that of the pole terms. At larger values of x_1 the seagull terms dominate. We calculated the values $\tilde{x}_1(Z)$ and the corresponding $\tilde{\omega}_1(Z)$. Since the seagull contribution increases rapidly in this energy region, we can assume that the seagull dominates for all $\omega_1 > \tilde{\omega}_1$. Note that the part of the spectrum where $\omega_1 - \omega_2 \sim \omega_1 \gg I$, that is, where the energies of the ejected electrons $\varepsilon \gg I$ is still determined by the pole terms.

At $\omega_2 \ll \omega_1, I$ the pole terms exhibit an infrared divergent behavior $d\sigma(\omega_1, \omega_2)/d\omega_2 \sim 1/\omega_2$. This is a manifestation of the general low-energy theorem [22]. Similar divergent terms are contained in the radiative corrections to the photoeffect. In the total cross section of photoionization (i.e., in the sum of the cross section of the photoeffect with the radiative corrections and that of the Compton scattering), the divergent terms cancel [22]. In [23] this was shown explicitly for the case of the high-energy photons. We shall not carry out this program for the low-energy case. Instead of this we assume that the detector of the ejected electrons can distinguish the electron with the largest available energy $\varepsilon_m = \omega_1 - I$ from that with the energy $\varepsilon_\lambda < \varepsilon_m$, $\varepsilon_m - \varepsilon_\lambda \ll \varepsilon_m$, but cannot distinguish the electrons with the energies ε in the interval $\varepsilon_\lambda < \varepsilon < \varepsilon_m$ from those with the energy ε_m . Thus, all the events of the Compton scattering with the energies $\varepsilon_\lambda < \varepsilon < \varepsilon_m$ will be counted as those of the photoeffect. This is equivalent to the introduction of a

cutoff $\omega_2 > \omega_\lambda = \omega_1 - I - \varepsilon_\lambda$ in the spectrum of the ejected photons. We investigate the dependence of our results on the actual value of ω_λ .

For the energies, restricted by Eq. (2), the Compton scattering cross section is still much smaller than that of the photoeffect. The energy behavior of the ratio of the two cross sections for several values of Z are presented in the paper.

Our calculations are carried out for a single-electron ion. We expect the main features of our analysis to be true for the K -shell electrons of the atoms. In this case all the cross sections should be multiplied by a factor 2, corresponding to the number of electrons in the K shell.

II. GENERAL EQUATIONS

The general equation for the differential cross section is

$$d\sigma = \frac{2\pi}{2\omega_1} \delta(\varepsilon + \omega_2 - \omega_1 - I) |M|^2 \frac{d^3p}{(2\pi)^3} \frac{d^3k_2}{(2\pi)^3} \frac{1}{2\omega_2}.$$

Here p is the linear momentum of the ejected electron and M is the amplitude of the process. In expression $|M|^2$ averaging (summation) over polarizations of the incoming (outgoing) photons is assumed. Using the delta function for integration over the electron energies, we can write

$$d\sigma = \frac{1}{(2\pi)^3} \frac{\omega_2}{\omega_1} m p |M|^2 \frac{d\Omega_e}{4\pi} \frac{d\Omega_\gamma}{4\pi} d\omega_2. \quad (4)$$

Here, $\Omega_{e(\gamma)}$ are the solid angles of the final-state particles. This equation is widely used in the papers on the Compton scattering from the bound electrons (see, e.g., [14]).

The amplitude can be presented as the sum of the pole and seagull contributions, denoted as M_P and M_{SG} correspondingly,

$$M = M_P + M_{SG}. \quad (5)$$

The pole terms are due to inclusion of the interaction, described by the first term on the right-hand side of Eq. (1) in the second order of the perturbation theory. They are given by the standard expressions (see, e.g., [22]),

$$M_P = M_{Pa} + M_{Pb}; \quad M_{Pa} = \langle \psi_f | V^{*(2)} G(p_a) V^{(1)} | \psi_i \rangle,$$

with $\psi_{i(f)}$ standing for the electron wave function in the initial (final) state; G is the Green function of the electron, $p_a = \sqrt{2m(\omega_1 - I)}$; $V^{(j)}$ describe interaction of the photon ($j = 1, 2$) with the electron. We employ the velocity gauge with $V^{(j)} = -(4\pi\alpha)^{1/2} i[(\mathbf{e}_j \cdot \nabla)/m] e^{i(\mathbf{k}_j \cdot \mathbf{r})}$. The contribution M_{pb} can be obtained by changing $\mathbf{e}_1 \leftrightarrow \mathbf{e}_2$, $\mathbf{k}_1 \leftrightarrow -\mathbf{k}_2$, $\omega_1 \leftrightarrow -\omega_2$ in the expression for M_{pa} . For further evaluation we shall present the contributions M_{pa} and M_{pb} in momentum space.

$$\begin{aligned} M_{Pa} &= 4\pi\alpha \int \frac{d^3f_1}{(2\pi)^3} \frac{d^3f_2}{(2\pi)^3} \langle \psi_p | \mathbf{f}_1 - \mathbf{k}_2 \rangle \frac{(\mathbf{e}_2 \cdot \mathbf{f}_1)}{m} \\ &\quad \times \langle \mathbf{f}_1 | G(p_a) | \mathbf{f}_2 \rangle \frac{(\mathbf{e}_1 \cdot \mathbf{f}_2)}{m} \langle \mathbf{f}_2 - \mathbf{k}_1 | \psi_{1s} \rangle; \\ M_{Pb} &= 4\pi\alpha \int \frac{d^3f_1}{(2\pi)^3} \frac{d^3f_2}{(2\pi)^3} \langle \psi_p | \mathbf{f}_1 + \mathbf{k}_1 \rangle \frac{(\mathbf{e}_1 \cdot \mathbf{f}_1)}{m} \\ &\quad \times \langle \mathbf{f}_1 | G(p_b) | \mathbf{f}_2 \rangle \frac{(\mathbf{e}_2 \cdot \mathbf{f}_2)}{m} \langle \mathbf{f}_2 + \mathbf{k}_2 | \psi_{1s} \rangle; \\ p_a &= \sqrt{2m(\omega_1 - I)}; \quad p_b = i\sqrt{2m(\omega_2 + I)}. \end{aligned} \quad (6)$$

In Eq. (6) ψ_{1s} and $\psi_{\mathbf{p}}$ are the Coulomb wave functions of the $1s$ electron and of the continuum electron with asymptotic linear momentum \mathbf{p} , G is the Coulomb Green function, and $\mathbf{e}_{1(2)}$ are vectors of polarization of the photons. The electron functions in Eq. (6) are just the Fourier transforms of those in coordinate space: $\psi_{\mathbf{p}}(f) = \int \phi_{\mathbf{p}}(r) e^{-i(\mathbf{f} \cdot \mathbf{r})} d^3r$, etc.

The seagull contribution is

$$M_{\text{SG}} = \frac{4\pi\alpha(\mathbf{e}_1 \cdot \mathbf{e}_2)}{m} \int \frac{d^3f}{(2\pi)^3} \langle \psi_{\mathbf{p}} | \mathbf{f} \rangle \langle \mathbf{f} - \mathbf{k} | \psi_{1s} \rangle, \quad (7)$$

with $\mathbf{k} = \mathbf{k}_1 - \mathbf{k}_2$. One can see immediately that for $\mathbf{k} = \mathbf{0}$ the amplitude M_{SG} vanishes due to orthogonality of the wave functions. Actually, Eqs. (5)–(7) have been first obtained in [24].

The Coulomb Green function can be represented in various forms. We use the one, obtained in [20]. Employing the equations, obtained in [17], we present the pole amplitudes $M_{Pa(b)}$ in terms of one-dimensional integrals. These equations can be obtained from those of [21] by changing \mathbf{k}_2 to $-\mathbf{k}_2$ and ω_2 to $-\omega_2$. Employing the dipole approximation (i.e., putting in the arguments of the wave functions $\mathbf{k}_1 = \mathbf{k}_2 = \mathbf{0}$), neglecting thus the contributions of the order ω_1^2/η^2 , one obtains [14]

$$M_{Pa(b)} = 32\pi^2 r_e N N_p \eta^{-3} ((\mathbf{e}_1 \cdot \mathbf{e}_2) F_{a(b)} + (\mathbf{e}_1 \cdot \mathbf{n})(\mathbf{e}_2 \cdot \mathbf{n}) \Phi_{a(b)}), \quad (8)$$

where $F_{a,b}$ and $\Phi_{a,b}$ are certain functions of x_1 and x_2 . Here, $r_e = \alpha/m$ is the electron radius, $\mathbf{n} = \mathbf{p}/p$, $N = \sqrt{\eta^3/\pi}$, and $N_p = \sqrt{2\pi\xi/[1 - \exp(-2\pi\xi)]}$ are the normalization factors of the $1s$ and continuum electrons, and $\xi = \eta/p$ is the Sommerfeld parameter of the ejected electron. Introducing, also,

$$x_1 = \frac{\omega_1}{I}; \quad x_2 = \frac{\omega_2}{I}; \quad \zeta = \eta/p_a = (x_1 - 1)^{-1/2},$$

we can write

$$F_a = -i \int_0^1 \frac{dy y f(y)}{\lambda(y)} A^{-1+i\xi} B^{-1-i\xi}; \quad (9)$$

$$\Phi_a = 2 \frac{(1-i\xi)(2-i\xi)}{\xi^2} \int_0^1 dy y f(y) A^{-3+i\xi} B^{-i\xi}.$$

Here,

$$\lambda(y) = [x_1(1-y) - 1]^{1/2}; \quad f(y) = \left(\frac{i\zeta - 1}{i\zeta + 1} \frac{\zeta\lambda + 1}{\zeta\lambda - 1} \right)^{i\xi},$$

while $A = \lambda^2 - \xi^{-2}$; $B = (\lambda + \xi^{-1})^2$. Equations for F_b and Φ_b can be obtained by changing the lower index a to b and x_1 to $-x_2$.

The seagull term can be calculated explicitly (see Appendix):

$$M_{\text{SG}} = 32\pi^2 \alpha^2 Z N N_p (\mathbf{e}_1 \cdot \mathbf{e}_2) \left(\frac{1-i\xi}{A_0} + \frac{1+i\xi}{B_0} \right) \times A_0^{-1+i\xi} B_0^{-i\xi}, \quad (10)$$

with $A_0 = -\eta^2 - (\mathbf{p} - \mathbf{k})^2$, $B_0 = -k^2 + (p + i\eta)^2$. In contrast to the situation with the pole terms we cannot put $\mathbf{k} = \mathbf{0}$, since at $\mathbf{k} = \mathbf{0}$ the amplitude $M_{\text{SG}} = 0$. This is due to orthogonality of the wave functions in the integral on the

right-hand side of Eq. (7). Neglecting the terms of the relative order ω_1^2/η^2 we find

$$M_{\text{SG}} = 64\pi^2 \alpha^2 Z N N_p \eta^{-6} (\mathbf{e}_1 \cdot \mathbf{e}_2) (\mathbf{p} \cdot \mathbf{k}) \frac{1-i\xi}{(x_p + 1)^3} \times \exp[-2\xi \arctan(1/\xi)]. \quad (11)$$

Here, we introduced

$$x_p = \frac{\varepsilon}{I} = x_1 - x_2 - 1, \quad (12)$$

which is the energy of the outgoing electron ‘‘in units’’ of the binding energy.

III. ENERGY DISTRIBUTIONS

Using Eqs. (8) and (11) and carrying out the angular integrations, we find equations for the energy distributions. One can see from Eqs. (8) and (11) that the pole terms do not interfere with the seagull ones. Thus, the energy distribution can be represented by Eq. (3).

A. Contribution of the pole terms

Employing Eqs. (8) and (11) we obtain

$$\frac{1}{\sigma_{Th}} \frac{d\sigma_P}{dx_2} = 32 \frac{x_2}{x_1} X(x_1, x_2) \frac{1}{1 - \exp(-2\pi\xi)}, \quad (13)$$

with

$$X = |F|^2 + \frac{2}{3} \text{Re}(F^* \Phi) + \frac{1}{3} |\Phi|^2; \quad F = F_a + F_b; \quad \Phi = \Phi_a + \Phi_b, \quad (14)$$

while

$$\sigma_{Th} = \frac{8\pi}{3} r_e^2$$

is the nonrelativistic limit of the Compton scattering cross section on a free electron, known also as the Thomson cross section.

The Low theorem [25], [22] predicts the energy distribution of soft photons with $\omega_2 \ll I, \omega_1$,

$$\frac{d\sigma_P(\omega_1, \omega_2)}{d\omega_2} = \sigma_{ph}(\omega_1) w(\omega_1, \omega_2); \quad w(\omega_1, \omega_2) = \alpha \frac{2}{3\pi} \frac{p^2}{m^2} \frac{1}{\omega_2}. \quad (15)$$

Here, σ_{ph} is the photoeffect cross section, w describes ejection of the soft photon, p is the linear momentum of the photoelectron, $p^2 = 2m(\omega_1 - I)$. This can be obtained also by straightforward evaluation of Eq. (13) in the limit $x_2 \rightarrow 0$. In [21] Eq. (15) was obtained explicitly for the case of the two-photon absorption (with w the probability of the induced absorption). The infrared behavior of the Compton amplitude was first mentioned in [14]. An analysis of the soft photon ejection in the Compton scattering on bound electrons in the relativistic case was given in [26].

Examples of the energy distributions for several values of x_1 are given in Fig. 1. In order to find the region of validity of the low-energy behavior $d\sigma_P/dx_2 \sim 1/\omega_2$ we show also the function $x_2/\sigma_{Th} d\sigma_P/dx_2$ (dashed line in Fig. 1). Deviation of this function from a constant value corresponds to deviation of the energy distribution from the behavior, described by

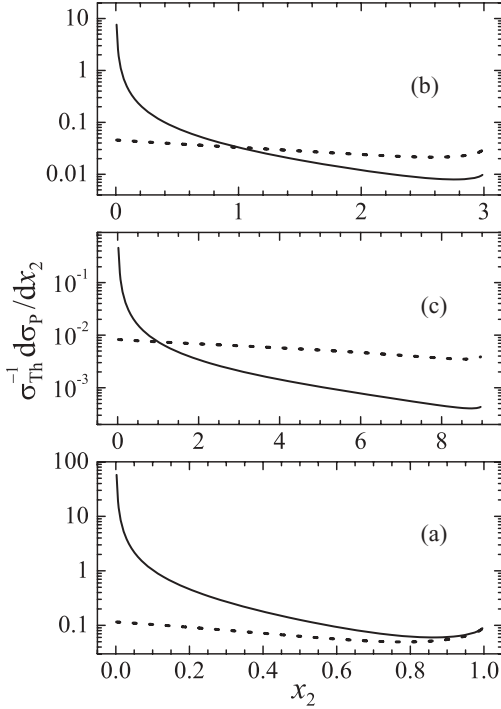


FIG. 1. The photon energy distributions, provided by Eq. (13), for $x_1 = 2, 4, 10$ are shown by the solid lines in (a)–(c), correspondingly. The dashed lines show the function $(x_2/\sigma_{Th})d\sigma_p/dx_2$. Their deviations from horizontal lines correspond to deviations of the energy distributions from the behavior, described by Eq. (15).

Eq. (15). One can see that Eq. (15) is true with good accuracy in a large part of the energy interval.

In the case $\omega_1 \gg I$ ($x_1 \gg 1$) we can distinguish the two regions of the spectrum. These are $x_1 - x_2 \sim 1 \ll x_1$, corresponding to slow outgoing electrons with the energies $\varepsilon \sim I$, and $x_1 - x_2 \sim x_1 \gg 1$, with the fast electrons carrying the energies $\varepsilon \sim \omega_1 \gg I$. Each of the amplitudes $F_{a,b}$ and $\Phi_{a,b}$ treated separately peaks at $\varepsilon \sim I$. However, a large compensation takes place in the sums $F_a + F_b$ and $\Phi_a + \Phi_b$. To demonstrate this, note that in the case $x_{1,2} \gg 1$ the Coulomb Green functions can be replaced by free propagators G_0 , since $p_{a,b} \gg \eta$ in Eq. (6). Presenting $\langle \mathbf{f} | G_0(p_j) | \mathbf{f}_1 \rangle = 2m\delta(\mathbf{f} - \mathbf{f}_1)/(p_j^2 - f^2)$, ($j = a, b$) and noting that the integrals on the right-hand sides of Eq. (6) are saturated by $f \sim \eta$, one can see that the leading contributions to the amplitudes $F_a + F_b$ and $\Phi_a + \Phi_b$ cancel. Finally, for all ω_1 the energy distribution drops while the electron energy diminishes.

Note that one can obtain the energy distributions also by integration of the double differential distributions obtained in [19]. These distributions were calculated with the Coulomb propagator obtained in [27]. The matrix elements were represented in terms of the Appel functions and computed by series summation. As expected, our results are close to those, based on the calculations of [19]; see Fig. 2. One can see that the deviations of the results obtained by using the two forms of the Coulomb propagator are of the same order as those of the data obtained by using its various representations in the

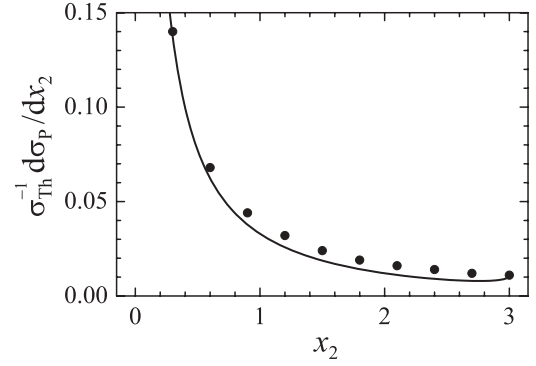


FIG. 2. The photon energy distribution at $x_1 = 4$, compared to that based on the results of [19]. Our results are shown by the solid line; the results of [19] are shown by dark dots.

related problem of the two-photon ionization of the hydrogen atom [28].

B. Seagull contribution

For the seagull contributions one can write

$$\frac{1}{\sigma_{Th}} \frac{d\sigma_{SG}}{dx_2} = \frac{64}{3} (\alpha Z)^2 x_1^2 V(x_p); \quad (16)$$

$$V(x_p) = \frac{1}{(x_p + 1)^5} \frac{\exp[-4\xi \arctan(1/\xi)]}{1 - \exp(-2\pi\xi)},$$

with $x_p = \varepsilon/I = x_1 - x_2 - 1$, $\xi = 1/x_p^{1/2}$. One can see that the explicit dependence on the nuclear charge Z and on the energy of incoming photon x_1 is factorized. The universal function $V(x_p)$ is presented in Fig. 3. One can see that it is concentrated at x_2 close to x_1 , corresponding to small $x_p \sim 1$. It reaches the maximum value at $x_p = 0.16$.

C. Differential cross sections

Following Eq. (3) they can be obtained as the sum of the energy distributions determined by Eqs. (13) and (16). Unlike the situation at $\omega_1 \sim I$, when the energy distributions depends only on x_2 and x_1 , in the general case it depends also on Z . However, there are some common features of the energy distributions.

All the spectrum curves have peaks at small x_2 determined by the pole terms and at small $x_1 - x_2$ determined by the seagull terms. These peaks manifest themselves even at $x_1 \sim 1$. The peak at small x_2 is due to the infrared divergence, expressed by Eq. (15), while the seagull terms have a sharp peak at small x_p .

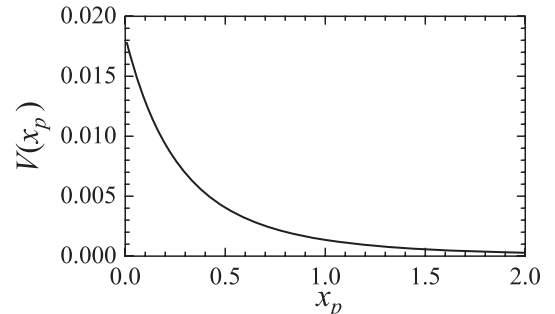


FIG. 3. The function $V(x_p)$ defined by Eq. (16).

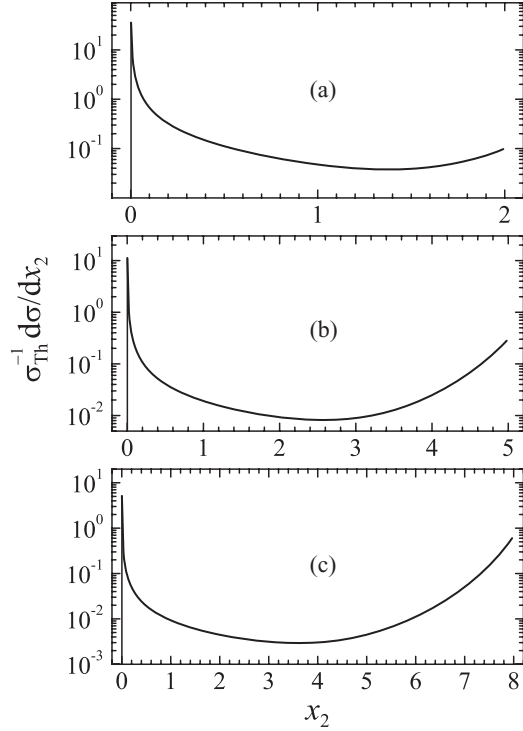


FIG. 4. Photon energy distributions for $Z = 20$ in these cases: (a) the total cross section is dominated by the pole terms ($x_1 = 2$); (b) the pole and seagull terms provide equal contributions to the cross section ($x_1 = 5$); (c) the cross section is dominated by the seagull term ($x_1 = 8$).

At $x_1 \gg 1$ the seagull peak at small x_p is more pronounced. On the other hand, the region $x_p \sim x_2 \sim x_1 \gg 1$ is dominated by pole terms. One can see this, describing the continuum and intermediate electrons in Eq. (6) by free functions. The contribution of the pole terms can be estimated as $M_p \sim r_e \psi_{1s}(p)$. On the other hand, the seagull term described by Eq. (7) can be estimated as $M_{SG} \sim r_e \psi_{1s}(p) \omega_1 / p$, being $\omega / p \sim (\omega / m)^{1/2}$ times smaller than M_p . Thus, the contribution of the seagull term to the energy distribution $d\sigma / d\omega_2$ at $\varepsilon \gg I$ provides a small correction of the order ω / m to that of the pole terms, and cannot be included in the nonrelativistic limit.

In Fig. 4 we provide examples of the photon energy distributions for $Z = 20$ at three characteristic values of x_1 . We shall return to this example in the next section.

IV. TOTAL CROSS SECTIONS

A. Energies $\omega_1 \sim I$

At these energies only the pole terms contribute to the total cross section. The latter can be obtained by numerical integration of Eq. (13).

One can see that the cross section $\sigma(\omega_1)$ is expected to have a local maximum at relatively small values of the ration $x_1 = \omega_1 / I$ close to unity. Indeed, one can see from Fig. 1 that a large part of the cross section can be estimated as coming from the region of the ejected soft photons, where the spectrum is described by Eq. (15). One can see that the upper limit of the values of x_2 where Eq. (15) is valid is certain $x_2 = c(x_1 - 1)$

with c an unknown coefficient. Thus, a large part of the cross section can be represented as

$$\frac{\sigma'_p(x_1)}{\sigma_{Th}} = U(x_1) \ln \left(\frac{c(x_1 - 1)}{\omega_\lambda / I} \right); \quad (17)$$

$$U(x_1) = \frac{4\alpha}{3\pi} \frac{I(x_1 - 1)}{m} \frac{\sigma_{ph}(x_1)}{\sigma_{Th}},$$

with the resolution threshold ε_λ determined in Sec. I. Using the well-known expression for the photoionization cross section (see, e.g., [29]), we find

$$U(x_1) = \frac{2^7}{3} \frac{x_1 - 1}{x_1^4} \frac{\exp[-4\zeta \arctan(1/\zeta)]}{1 - \exp(-2\pi\zeta)}. \quad (18)$$

Here $\zeta = (x_1 - 1)^{-1/2}$ is the Sommerfeld parameter of photoelectron. Now we can look for the values of ω_1 where the ratio $\sigma'_p(x_1) / \sigma_{Th}$ (17) reaches its maximum value. Assuming that the resolution threshold is proportional to the energy of photoelectron, that is,

$$\omega_\lambda = \lambda(\omega_1 - I), \quad \lambda \ll 1, \quad (19)$$

we find that the contribution (17) obtains its largest value at $x_1 = \omega_1 / I = 1.56$ [see Fig. 5(a)]. If ω_λ does not depend on ω_1 (or depends on it in a more complicated way), the maximum of (17) is shifted from this value.

The results of numerical calculations, shown in Fig. 5(a) confirm these estimations. In Fig. 5(b) we present the results

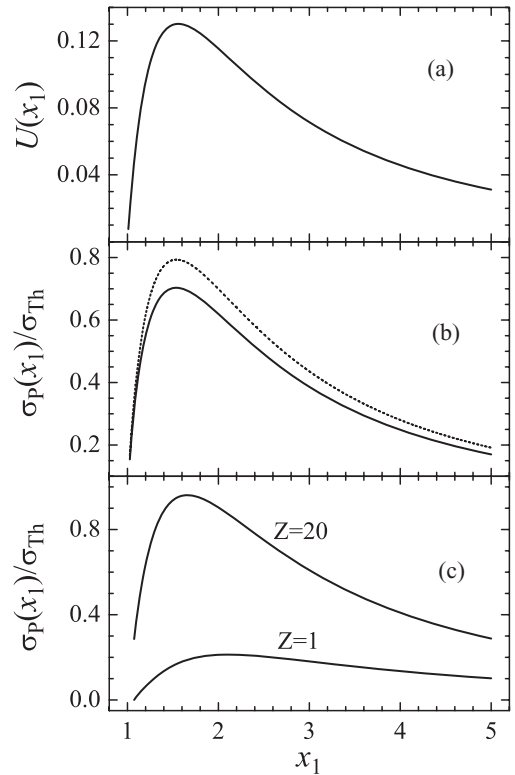


FIG. 5. The total cross section at $x_1 \sim 1$. Figure 5(a) shows the function $U(x_1)$ defined by Eq. (18). Figure 5(b) illustrates the dependence of the contribution $\frac{\sigma'_p(x_1)}{\sigma_{Th}}$ defined by Eq. (17) on the actual value of λ , introduced by Eq. (19). Solid line, $\lambda = 2 \times 10^{-3}$; dashed line, $\lambda = 10^{-3}$. Figure 5(c) shows the total cross section for $Z = 1$ and $Z = 20$.

for the value ω_λ given by Eq. (19) with two different values of λ .

If ω_λ does not depend on ω_1 we can write

$$\frac{\sigma_P(x_1)}{\sigma_{Th}} = W(x_1) + U(x_1) \ln Z^2; \quad (20)$$

$$W(x_1) = \int_{\omega_\lambda/I_1}^{x_1-1} dx_2 \frac{d\sigma_P(x_1, x_2)}{\sigma_{Th} dx_2},$$

with $I_1 = m\alpha^2/2 = 13.6$ eV the binding energy for $Z = 1$. The distribution $d\sigma_P(x_1, x_2)/\sigma_{Th} dx_2$ is determined by Eq. (13). We assume $\omega_\lambda = 1$ eV [7], and present for illustration the function $W(x_1)$ [$\sigma_P(x_1)/\sigma_{Th} = W(x_1)$ for $Z = 1$] and the function $\sigma_P(x_1)/\sigma_{Th}$ for $Z = 20$ [Fig. 5(c)].

B. The case $\omega_1 \gg I$

Here, we must add the contribution of the seagull term to that of the pole term. Using Eq. (16), we find

$$\frac{\sigma_{SG}}{\sigma_{Th}} = \frac{64}{3} (\alpha Z)^2 x_1^2 \int_0^{x_1-1} dx_p V(x_p). \quad (21)$$

One can see that the integral on the right-hand side of Eq. (21) is saturated at $x_p \sim 1$ and at $x_1 \gg 1$ does not depend on the actual value of the upper limit. Thus, it can be replaced by $\int_0^\infty dx_p V(x_p) = 6.6 \times 10^{-3}$. This leads to the cross section,

$$\frac{\sigma_{SG}}{\sigma_{Th}} = 0.14 (\alpha Z)^2 x_1^2 = 0.56 \frac{\omega_1^2}{\eta^2}. \quad (22)$$

One can see that while the contribution of the pole terms drops with x_1 at $x_1 \gg 1$, the contribution of the seagull terms, being negligibly small at $x_1 \sim 1$, increases at larger x_1 until Eq. (2) is true. At certain value \tilde{x}_1 the two contributions become equal. The curve \tilde{x}_1 , thus, separates the regions of the dominance of the pole and seagull terms. The curve \tilde{x}_1 is shown in Figs. 6(a) and 6(b). The corresponding curve for

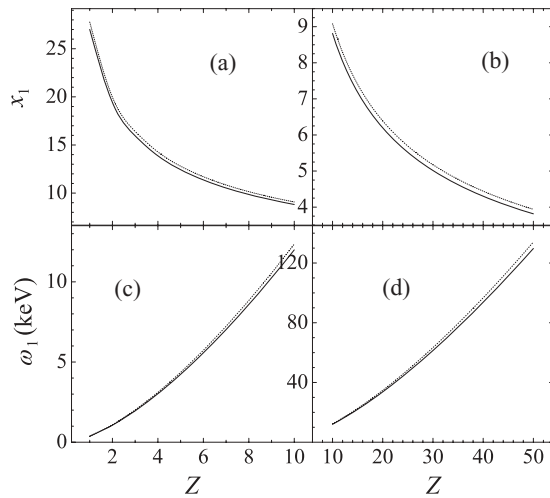


FIG. 6. The border between the regions of dominant pole or seagull terms. For the values of x_1 above the curve $\tilde{x}_1(Z)$ in (a) and (b) or for the values ω_1 above the curve $\tilde{\omega}_1(Z)$ in (c) and (d), the seagull terms dominate. For the values below these curves, the cross sections are determined by the pole terms. Solid line, $\lambda = 2 \cdot 10^{-3}$; dashed line, $\lambda = 10^{-3}$.

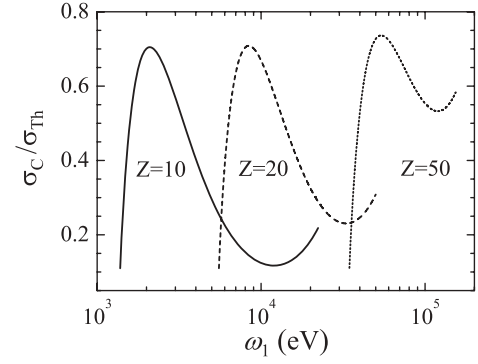


FIG. 7. The energy dependence of the Compton scattering cross section for several values of Z . Solid line, $Z = 10$; dashed line, $Z = 20$; dotted line, $Z = 50$.

the absolute value of the photon energy $\tilde{\omega}_1(Z)$ is shown in Figs. 6(c) and 6(d). The energy dependence of the Compton scattering cross section for several values of the nuclear charge is shown in Fig. 7.

V. SUMMARY

We calculated the energy distributions and the total cross section for the Compton scattering on the K -shell electrons in the low-energy region, determined by Eq. (2), that is, for the case when the wavelength of the photons is much smaller than the size of the K shell. All the electrons were described by the nonrelativistic Coulomb functions. The results are true for the single-electron ions with the nuclear charge Z . We expect also that they reproduce the main features of the process on the many-electron ions and atoms.

We calculated the contribution of the pole terms by using a close representation for the Coulomb Green function. In the lowest order of expansion in powers of η^2/ω^2 the pole and seagull terms do not interfere.

At the photon energies of the order of the K -shell binding energies $\omega_1 \sim I = m(\alpha Z)^2/2$ the seagull terms provide a small correction of the order $(\alpha Z)^2$ to the pole terms and cannot be taken into account in the framework of the nonrelativistic approach. In this case, the photon spectrum drops with an increase of the ejected photon energies. As one can see in Fig. 1, the low-energy Eq. (15) describes most part of the spectrum at $\omega_1 \sim I$. At $\omega_1 \gg I$, the high-energy part of the photon spectrum $\omega_1 - \omega_2 \sim I$, corresponding to slow ejected electrons with energies $\varepsilon \sim I$, is dominated by the seagull terms (Fig. 3). All the other parts of the spectrum are determined by the pole terms. Examples of the energy distribution are presented in Fig. 4.

The total cross sections obtain maxima at energies $\omega_1 \sim (1.5-2)I$, reaching the value of 0.5–1 barn (Fig. 5). Here the cross sections are determined by the pole terms. The contribution of the pole terms drops at larger energies. However, at $\omega_1 \gg I$ the contribution of the seagull terms, which increases with ω_1 , becomes important. At certain value $\tilde{\omega}_1 \gg I$, the pole and seagull terms provide equal contribution, and at larger values of ω_1 the seagull terms dominate. The values $\tilde{\omega}_1(Z)$ are presented in Fig. 6.

The present analysis can be useful in connection with the laser-assisted and laser-induced processes, which are

much discussed nowadays [30]. For example, in Ref. [31], the authors considered the laser-field-assisted high-energy Compton scattering on the bound electron with the energies of the ejected electrons $\varepsilon \gg I$. They took into account only the seagull terms. However, it follows from the present analysis that for $\omega_1 \ll \eta$ this part of the spectrum is described by the pole terms. This provides additional restrictions for the energy region where the approach developed in [31] is valid.

APPENDIX

A convenient technique of evaluation of the matrix elements, containing the Coulomb functions, was worked out in [20]. The Coulomb function of $1s$ state can be written as

$$\varphi_{1s}(r) = N \left(-\frac{\partial}{\partial \eta} \right) V_\eta; \quad N = \left(\frac{\eta^3}{\pi} \right)^{1/2}; \quad V_\eta = \frac{e^{-\eta r}}{r}, \quad (\text{A1})$$

while in momentum space,

$$\psi_{1s}(\mathbf{f} - \mathbf{k}) = N \left(-\frac{\partial}{\partial \eta} \right) \langle \mathbf{f} | V_\eta | \mathbf{k} \rangle. \quad (\text{A2})$$

The wave function of the continuum electron with asymptotic linear momentum p can be written as

$$\psi_{\mathbf{p}}(\mathbf{f}) = N_p \left(-\frac{\partial}{\partial v} \right) \hat{J}_x \langle \mathbf{p}(1-x) | V_{v-ipx} | \mathbf{f} \rangle, \quad v = 0, \quad (\text{A3})$$

with the normalization factor N_p defined in the text and

$$\hat{J}_x = \int \frac{dx}{x} \left(\frac{-x}{1-x} \right)^{i\xi}; \quad \xi = \frac{\eta}{p}. \quad (\text{A4})$$

Here, the contour of integration is a closed loop encircling the cut between the branching points $x = 0$ and $x = 1$ in the counterclockwise direction.

Now the integral in Eq. (7) is

$$S = \int \frac{d^3 f}{(2\pi)^3} \langle \psi_{\mathbf{p}} | \mathbf{f} \rangle \langle \mathbf{f} - \mathbf{k} | \psi_{1s} \rangle \\ = NN_p \left(-\frac{\partial}{\partial \eta} \right) \left(-\frac{\partial}{\partial v} \right) \hat{J}_x \langle \mathbf{p}(1-x) | V_{v-ipx} V_\eta | \mathbf{k} \rangle. \quad (\text{A5})$$

One can see that

$$\left(-\frac{\partial}{\partial v} \right) V_{v+a} V_\eta = V_{v+a+\eta}, \quad (\text{A6})$$

and, thus,

$$S = NN_p \left(-\frac{\partial}{\partial \eta} \right) \hat{J}_x \langle \mathbf{p}(1-x) | V_{\eta-ipx} | \mathbf{k} \rangle. \quad (\text{A7})$$

The only singularity of the integrand in the integral over x in (A7) is the single pole of the matrix element $\langle \mathbf{p}(1-x) | V_{\eta-ipx} | \mathbf{k} \rangle$. Its residue provides

$$S = NN_p \left(-\frac{\partial}{\partial \eta} \right) \frac{4\pi}{A_0} \left(\frac{A_0}{B_0} \right)^{i\xi}, \quad (\text{A8})$$

with A_0 and B_0 defined in the text just below Eq. (10). This leads to Eq. (10) for the seagull term.

-
- [1] G. Wentzel, *Z. Phys.* **43**, 1 (1927).
[2] V. Florescu and R. H. Pratt, *Phys. Rev. A* **80**, 033421 (2009).
[3] R. H. Pratt, L. A. LaJohn, V. Florescu, T. Suric, B. K. Chatterjee, and S. C. Roy, *Radiat. Phys. Chem.* **79**, 124 (2010).
[4] F. Schnaidt, *Ann. Physik (Leipzig)* **21**, 89 (1934).
[5] V. G. Gorshkov, A. I. Mikhailov, and S. G. Sherman, *Sov. Phys. JETP* **37**, 572 (1973); **50**, 15 (1979).
[6] P. M. Bergstrom Jr., T. Surić, K. Pisk, and R. H. Pratt, *Phys. Rev. A* **48**, 1134 (1993).
[7] P. P. Kane, *Phys. Rep.* **218**, 67 (1992); *Radiat. Phys. Chem.* **50**, 31 (1997).
[8] S. Pasic and K. Ilakovac, *Radiat. Phys. Chem.* **75**, 1683 (2006).
[9] S. H. Southworth, R. W. Dunford, D. L. Ederer, E. P. Kanter, B. Krassig, and L. Young, *Radiat. Phys. Chem.* **70**, 655 (2004).
[10] A. Becker and F. H. M. Faisal, *Laser Physics* **13**, 430 (2003).
[11] S. A. Novikov and A. N. Hopersky, *J. Phys. B* **35**, L339 (2002).
[12] P. Eisenberger and P. Platzman, *Phys. Rev. A* **2**, 415 (1970).
[13] I. G. Kaplan and G. L. Yudin, *Sov. Phys. JETP* **42**, 4 (1976).
[14] M. Gavrila, *Phys. Rev. A* **6**, 1348 (1972).
[15] M. Gavrila, *Lett. Nuovo Cimento* **2**, 180 (1969).
[16] S. Klarsfeld, *Lett. Nuovo Cimento* **2**, 548 (1969).
[17] V. G. Gorshkov and V. S. Polikanov, *Sov. Phys. JETP Letters* **9**, 279 (1969).
[18] L. P. Rapoport, B. A. Zon, and L. N. Manakov, *Sov. Phys. JETP* **29**, 220 (1969).
[19] M. Gavrila, *Phys. Rev. A* **6**, 1360 (1972).
[20] V. G. Gorshkov, *Sov. Phys. JETP* **20**, 234 (1965).
[21] L. F. Vitushkin and A. I. Mikhailov, *Opt. Spectrosk.* **50**, 4 (1981).
[22] J. D. Bjorken and S. D. Drell, *Relativistic Quantum Mechanics* (McGraw-Hill, New York, 1964).
[23] J. McEneaney and M. Gavrila, *Phys. Rev. A* **15**, 1537 (1977).
[24] H. A. Kramers and W. Heisenberg, *Z. Phys.* **31**, 681 (1925); I. Waller, *ibid.* **51**, 213 (1928).
[25] F. E. Low, *Phys. Rev.* **110**, 974 (1958).
[26] T. Suric, P. M. Bergstrom Jr., K. Pisk, and R. H. Pratt, *Rhys. Rev. Lett.* **67**, 189 (1991).
[27] J. Schwinger, *J. Math. Phys.* **5**, 1606 (1964).
[28] E. Karule, *Adv. At. Mol. Phys.* **26**, 265 (1990).
[29] H. A. Bethe and E. E. Salpeter, *Quantum Mechanics of One- and Two-Electron Atoms* (Dover Publications, New York, 2008).
[30] D. B. Miloshević and F. Ehlötzky, *Adv. At. Mol. Phys.* **49**, 373 (2003).
[31] A. B. Voitkiv, N. Grün, and J. Ullrich, *J. Phys. B* **36**, 1907 (2003).